2018

Comparison of Two Object-Oriented Modeling Environments for the Dynamic Simulations of a Residential Heat Pump

Viren Bhanot
"European Organization for Nuclear Research; University of Manchester", vbhanot@cern.ch

Rohit Dhumane
University of Maryland, United States of America, dhumane@umd.edu

Andrea Cioncolini
University of Manchester, andrea.cioncolini@manchester.ac.uk

Paolo Petagna
European Organization for Nuclear Research, paolo.petagna@cern.ch

Jiazhen Ling
University of Maryland, College Park, United States of America, jiazhen@umd.edu

See next page for additional authors

Comparison of Two Object-Oriented Modeling Environments for the Dynamic Simulations of a Residential Heat Pump

Viren BHANOT[1, 2]*, Rohit DHUMANE[3], Paolo PETAGNA[1], Andrea CIONCOLINI[2], Jiazhen LING[3], Vikrant AUTE[3], Reinhard RADERMACHER[3]

[1]European Organization for Nuclear Research, EP-DT-FS,
Geneva, Switzerland
Email: vbhanot@cern.ch, paolo.petagna@cern.ch,

[2]University of Manchester, Department of Mechanical, Aerospace and Civil Engineering
Manchester, United Kingdom
Email: andrea.cioncolini@manchester.ac.uk

[3]University of Maryland, College Park, Department of Mechanical Engineering,
College Park, Maryland, United States
Email: dhumane@umd.edu, jiazhen@umd.edu, vikrant@umd.edu, raderm@umd.edu

* Corresponding Author

ABSTRACT

Object-oriented physical-modeling platforms offer a productive way of performing dynamic simulations of thermofluid systems. They simplify component development and code reuse and abstract away the complexities of sorting the resultant equations. In this study, we compare two platforms of this type: Dymola and EcosimPro. We use these platforms to conduct a realistic exercise of modeling and simulating a relatively complex residential heat pump in both heating and cooling modes and comparing the results against measured data. The heat pump used for measurements is a 3-ton residential R-410A unit. The parameters compared are the refrigerant pressures and temperatures, the compressor power consumption, the indoor unit air-side capacity and the heat exchanger air outlet temperatures. The two platforms prove to be similarly capable in predicting the performance of the heat pump, with deviations in accumulated capacities and power consumption being within 20% of measured values. Some differences are caused by fact that the Dymola model uses REFPROP-based curve fits for evaluation of fluid properties, while EcoSimPro uses a lookup table for faster evaluation and avoids zero mass flow cases by providing a small artificial mass flow rate in off-cycles. Implications of these assumptions and improvements on simulation speed are discussed.

Keywords: Modelica; Dymola; EcosimPro; Dynamic simulations; Heat pump; Object oriented modelling

1. INTRODUCTION

There are several benefits of conducting dynamic simulations of thermofluid systems. Simulations performed on a computer are less expensive compared to developing a test facility for such purposes. Iterating between different design alternatives can also be done faster. Such simulations assist the designer in gaining a deeper understanding of system behavior; "what-if" questions can be answered, and parameters not easily measured can be investigated (such as the state of the fluid when it is in two-phase or the mass inventory inside individual components). System behavior in unsafe conditions for testing can be simulated to improve safety and reliability.

Several facets of thermofluid systems, however, make transient simulations challenging: the models often exhibit stiffness characteristics, and the resulting set of equations are typically Differential Algebraic Equations (DAEs) rather than Ordinary Differential Equations (ODEs), which are more complicated for the solver (Petzold, 1982). In the past, modelers looking to simulate such systems would be required to not just develop the component models, but also implement the associated numerical methods to solve the models.

The proliferation of tools such as Matlab/Simulink and TRNSYS gave modelers access to built-in solvers capable of handling stiff systems and DAEs. Simulink has seen wide adoption for simulating thermofluid systems (Bhanot et al., 2016; Eldredge et al., 2005; Hossin et al., 2001). Simulink is a block-based modeling platform where the individual blocks contain the component code, and signals carry the associated variables between such blocks.

The preceding two decades, however, have witnessed a considerable gain in popularity of an alternative paradigm of object-oriented modeling for physical systems. Platforms of such type encourage code reuse by allowing the equations to be stated in any order (often called 'acausal' or non-causal modelling). Several limitations of the traditional approach make this newer approach attractive to designers. Simulink assumes that a system can be decomposed into block diagram format with causal interactions (Elmqvist et al., 1999). Several manual steps including differentiation are required to transform the equations to the form required by Simulink leading to inclusion of non-physical blocks like an Integrator. In addition, there is unidirectional data flow from inputs to outputs. By contrast, in acausal modeling-based blocks, the equations more closely resemble their mathematical form. Symbolic manipulations and index reduction operations are performed internally on a flat-code generated from the acausal models for faster run-times. Such platforms typically feature port connectors that can handle data flows associated with convective systems in a physical manner (for instance, dealing with splitting and mixing flows as well as reverse flows).

Another major benefit is that code reuse is much easier with object-oriented languages such as Modelica. Qiao et al. (2012) illustrated this point by performing a comparison between Simulink, SimScape and Modelica. A hypothetical four-component vapor-compression system was modeled and startup simulations were performed in each of the three platforms. SimScape is an equation-based extension of Simulink that seeks to adopt some of the facets of acausal modeling. Modelica is an object-oriented modeling language for modeling multi-domain physical systems. The authors noted that model reuse in Simulink was more challenging due to the fact that model topology can change completely when the model structure is changed.

In this study we perform a similar comparison between two object-oriented platforms: Dymola and EcosimPro. Dymola is a physical modeling environment originally developed at Lund University and now being maintained by Dassault Systèmes. It is a commercially available implementation of Modelica. EcosimPro is a proprietary tool developed by Empresarios Agrupados A.I.E originally for the European Space Agency and now sold to the general public. Previously, Muñoz et al. (2003) performed a comparative analysis between the two platforms for an angular velocity control system and found them to be similar in their capabilities. To the authors' knowledge, however, no such comparative study is available for thermofluid systems.

In this work, we use these platforms to model and simulate a residential heat pump. Heat pumps are vapor compression systems that can both heat and cool residential spaces. Such systems have relatively complex thermofluid dynamic behaviours and represent a good avenue to perform such an exercise. The simulation results were compared against experimental data collected from a test setup which is described in the next section.

2. TEST SETUP

The test unit is a 3-ton, R-410A heat pump for air-conditioning and space-heating applications. It was used in a previous study (Alabdulkarem et al., 2013) to investigate the impact of replacing R-410A with lower Global Warming Potential refrigerants ('drop-in' replacement). Both the indoor and outdoor units are round-tube, plate-fin heat exchangers. A single-stage scroll compressor circulates the refrigerant. In the cooling mode, a Thermostatic Expansion Valve (TXV) is used as the expansion device while in the heating mode a short-tube orifice with a fixed opening diameter is used. A reversing valve switches the flow direction. In this study, only results involving R-410A as the working fluid are considered.

A schematic of the experimental setup is shown in Figure 1. The outdoor unit was kept inside an environmental chamber with controlled temperature and humidity. Long pipes transported the refrigerant between the indoor and outdoor units, and the indoor unit was placed inside a closed air loop. The cyclic test conditions are derived from the ASHRAE Standard 116 (2010) and are listed in Table 1. Details of the measurement procedure may be found in Alabdulkarem et al. (2013).

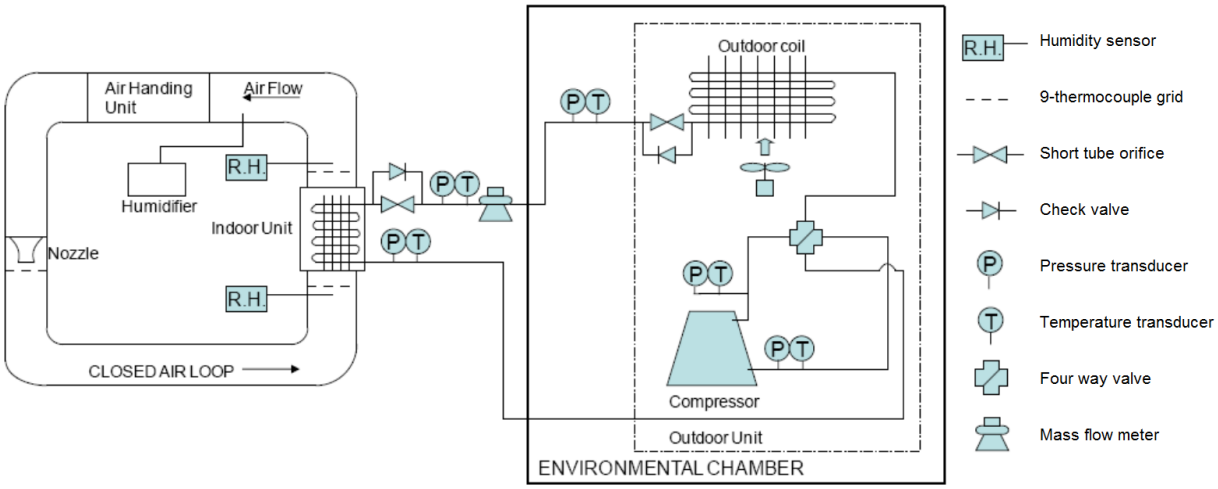

Figure 1. Test setup schematic.

Table 1. ASHRAE cyclic test conditions

Test Condition	Indoor Unit		Outdoor Unit	
	Dry Bulb	Wet bulb	Dry bulb	Wet bulb
D test	26.7°C	≤13.9°C	27.8°C	-
High Temperature Cyclic test	21.1°C	≤15.6°C	8.3°C	6.1°C

3. COMPONENT MODELING

The component models developed for this work derive are described in Ling et al. (2015) and Qiao et al. (2015). For the sake of brevity, detailed descriptions of the models have been eliminated. Instead, a brief overview of the most important details of the components are provided in this section.

3.1 Scroll Compressor

One of the simplifying assumptions commonly used in dynamic modeling is time scale abstraction. The dynamics of vapor compression systems are primarily dictated by the heat exchanger. The compressor and expansion device, with dynamics much faster than the heat exchanger, can thus be treated as quasi-steady state (Winkler, 2009). This has the advantage of simplifying the modeling of the compression process. On the other hand, the heat transfer within the compressor plays a significant role in determining system temperatures and, thus, must be accounted for. To this end, the compressor model has been divided into three parts: 1) the suction chamber, 2) the scroll-set, and 3) the discharge chamber.

In the suction chamber, the refrigerant enters from the inlet port and cools down the motor. Near the top of the chamber, the refrigerant is sucked into the scroll-set. The chamber has been modeled as a phase-separator, and the motor is modelled as a thermal mass that undergoes heat transfer with the vapor within the chamber.

A quasi-steady state model is used for the scroll set, and the mass flow rate and the power consumption are calculated using general equations of a scroll compressor (Winkler, 2009), shown in Equation (1). The discharge chamber has been modeled as a lumped volume. Both the natural-convective and the radiative heat transfer have been modeled for the discharge chamber shell. The Churchill and Chu (1975) correlation is used for the air-side heat transfer coefficient.

$$\dot{m} = \eta_{vol} . \rho_{in} . V . \frac{RPM}{60} \tag{1}$$

Where, V represents the displacement volume (m^3/rev) and RPM is the rotational speed.

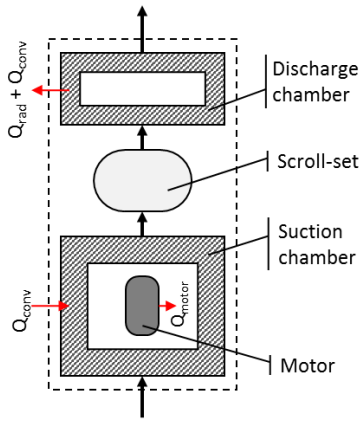

Figure 2. Scroll compressor schematic

3.2 Expansion Valves

Two types of expansion valves are present in the system, a thermostatic expansion valve (TXV) for the cooling mode and a short tube orifice for the heating mode. The orifice area is constant for the short tube, but varies with the evaporator outlet superheat for the TXV. Both models use the orifice equation to calculate the mass flow rate. The flow area of the TXV, however, is variable and depends on the force balance on the diaphragm. The sensor bulb pressure serves to open the valve, while the equalization pressure line and the spring offset closes the valve. Details of this model are given in Qiao et al. (2015).

3.3 Heat Exchangers

The heat exchangers dictate the dynamics of the vapor compression system and thus, more detailed physics is included in their models. The model is subdivided into three domains: refrigerant side, air side and the tube/fin thermal wall.

Refrigerant side

The refrigerant side is discretized using the finite volume method. The actual refrigerant circuitry in plate fin heat exchangers is complicated and is usually optimized for given geometry and air flow conditions. Modeling such complex configurations can involve expensive iterative calculations. Instead, the circuitry has been simplified as a bank-by-bank flow of refrigerant, as shown in Figure 3.

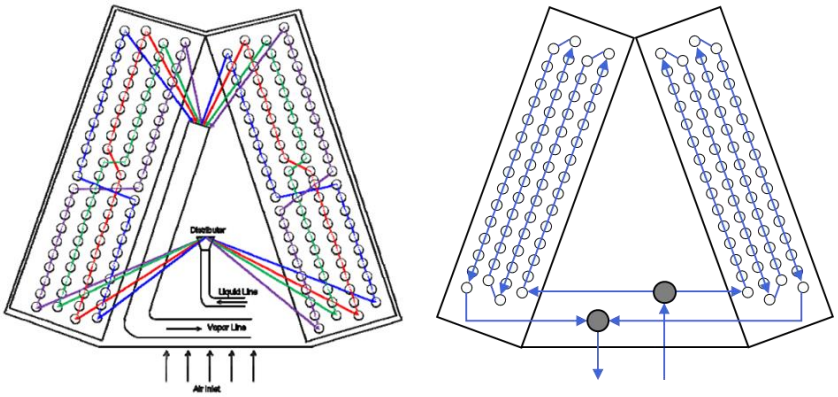

Figure 3. Heat exchanger circuitry, actual (left) and simplified (right).

The refrigerant flow in two-phase is assumed to be homogeneous. Pressure and specific enthalpy are used as the state variables. The staggered grid scheme is employed, wherein the control volume is discretized into thermal and momentum grids offset by half a cell width. The mass and energy balance are solved on the thermal grid and the momentum equation is solved on the momentum grid. The conservation equations for the j^{th} control volume, encased within the i^{th} and $(i+1)^{th}$ momentum volumes, are shown in Equations (2) and (3).

$$\frac{d\left(\rho V\right)_j}{dt} = V_j\left(\frac{\partial \rho_j}{\partial p_j}\frac{dp_j}{dt} + \frac{\partial \rho_j}{\partial h_j}\frac{dh_j}{dt}\right) = \dot{m}_i - \dot{m}_{i+1} \tag{2}$$

$$\frac{d\left(\rho u V\right)_j}{dt} = V_j\left(\frac{\partial \rho_j}{\partial p_j}h_j - 1\right)\frac{dp_j}{dt} + \left(\frac{\partial \rho_j}{\partial h_j} + \rho_j\right)\frac{dh_j}{dt} = m_i h_i - m_{i+1}h_{i+1} + Q_j \tag{3}$$

The momentum balance is assumed to be quasi-steady state, since dynamic pressure waves are not applicable. A quadratic relationship is assumed between the mas flow rate and the pressure drop, with nominal values provided as input for scaling, as shown in Equation (4).

$$\dot{m} = \dot{m}_0\sqrt{dP/dP_0} \tag{4}$$

Air side

The air side is modelled as 1-dimensional, quasi-steady flow. The air side heat transfer coefficient is calculated using the correlation by Wang et al. (2000). Performing an energy balance on the air-side gives Equation (5) which is used to calculate the air outlet temperature.

$$\dot{m}_{air}.c_{p,air}.(T_{air,in} - T_{air,out}) = \alpha_{air}.A_{o,eff}.(T_w - T_{air,in}) \tag{5}$$

Tube and fins

The tube and fins are discretized into the same number of volumes as the refrigerant flow, and a fin efficiency term is utilized to lump the tube and fins into a unified control volume. Heat conduction and radiation between the fins has been neglected. Energy is conserved for the thermal wall, and the difference in the heat transfer between the air side and the refrigerant side thus leads to a change in temperature of the wall.

3.4 Other Components

The heat pump includes a suction-line accumulator which prevents any potential liquid droplets from entering the compressor, and also stores excess refrigerant. The accumulator is modelled as a lumped control volume with liquid and vapor phase equilibrium (i.e., no mass or energy exchange) and also perfect separation of the two phases. The liquid level in accumulator is determined using the homogeneous density within the vessel and is used to establish the phase at the outlet port of the accumulator. Unless the liquid level is above the outlet port height, the outlet fluid is assumed to be saturated vapor.

Piping models have been developed that are similar to the heat exchanger model, although the air-side heat transfer is through natural convection only. Given the long piping in the test setup, a significant fraction of the system charge is held in the pipes. It is thus necessary to include them for improved charge prediction.

4. IMPLEMENTATION

4.1 Fluid Property Routines

Two different methods were used to calculate fluid properties. In EcosimPro, look-up tables derived using the REFPROP database (Lemmon et al., 2013) were used. In Dymola, an in-house enhancement (Aute & Radermacher, 2014) of the REFPROP database, in the form of polynomial curve fits, was used. To ensure that the different methods do not affect the comparison, an error analysis was undertaken. All five fluid regimes were compared: liquid region, saturated fluid (both vapor and liquid), two-phase region, vapor region and supercritical region.

For the saturated region, only one property is needed, and pressure was used as the independent variable. For the other regions, pressure and specific enthalpy were used as the independent variables. Temperature and density are compared to examine errors. Both the lookup table and the curve fit results were compared against REFPROP, treating REFPROP data as reference.

Details of the uncertainty from the use of the polynomial fits may be found in Aute and Radermacher (2014). The authors compared a variety of fluids, including R-410A, and found that the worst case Maximum Absolute Percentage Error (MAPE) was 0.1% for density calculation and the worst case Maximum Absolute Error (MAE) in saturation temperature was 6.79E-04 K.

For the lookup table uncertainty analysis, the saturation region was discretized into 1000 equidistant points starting at 3K above the triple point temperature, and up to 3K below the critical point. The number of discretization for pressure and enthalpy is 100. For the liquid region, the range is from the minimum temperature provided by REFPROP up to the liquid saturation line, for the two-phase region the domain is between the two saturation states, and for the vapor region, the domain is from the vapor saturations region to the maximum temperature for the fluid in REFPROP. For the supercritical region, the domain is from the critical point to the maximum fluid pressure in REFPROP.

The parameters used to compare the properties were the Maximum Absolute Error (MAE), the Maximum Absolute Percentage Error (MAPE) and the Absolute Mean Percentage Error (AAPE). The first parameter is useful for temperature comparison, the second parameter indicates the percentage error in the worst case while the final parameter quantifies the spread of the error across the domain. The results of the analysis are shown in Table 2.

The highest MAPE of 1.22% is found in the supercritical region. In the current application, however, the operating reduced pressures are low, and thus the refrigerant does not approach or exceed the critical point. The other errors are treated as acceptable, since both the MAPE and particularly the AAPE are less than 1%, indicating that the properties are reasonably close to the reference data. It is worth noting that lookup tables will always have greater errors than using the full equations of state or using refrigerant specific curve fits. The main benefit of such tables is increased simulation speed. If the nature of the system requires more accurate property routines (such as transcritical calculations) lookup tables may not have acceptable errors.

Table 2. EcosimPro fluid property error analysis

Property		**Sat. Liquid**	**Sat. Vapor**	**Liquid**	**Two-phase**	**Vapor**	**Supercritical**
Temperature (MAE) (K)		0.015	0.015	0.060	0.060	0.035	0.027
Density	MAPE (%)	0.340	0.816	0.223	0.244	0.209	1.222
	AAPE (%)	0.020	0.068	0.007	0.049	0.004	0.017

4.2 System Implementation

The component models were implemented on two separate machines. The specifications of the Dymola machine are as follows: Intel Xeon CPU (E3-1245, 3.50 GHz), 16 GB RAM, Windows 10 Enterprise (64 bit). The Dymola version number is: 'Dymola v2018 64 bit'. The EcosimPro simulations were conducted on a machine with the following specifications: Intel Core i7-6700 CPU (3.40 GHz), 8 GB RAM, Windows 7 Enterprise (64 bit). EcosimPro v5.6.0 64 bit was used. In general, the specifications of the machines were not found to be a limiting factor in the simulation speed. The solvers used for the comparison are the Radau IIa solver in Dymola and the IDAS_SPARSE solver in EcosimPro. The absolute and relative errors, along with the tolerance were set to 1.0E-6. While both platforms come equipped with the DASSL solver, the simulations with DASSL were found to proceed at impractically low speeds, and thus different solvers were used to expedite the simulations. Radau IIa solver, for instance, is noted to be especially fast during the off-cycle simulation with zero flow conditions (Dermont et al., 2016).

5. RESULTS AND DISCUSSION

5.1 Heating Mode Results

The heating mode results are shown in Figure 4. During the off-period before startup, the refrigerant accumulates in the coldest parts of the system. In the heating case, the outdoor ambient conditions are colder than indoors, thus the refrigerant collects in the outdoor components. Specifically, a significant amount is stored in the accumulator.

Just before startup, the refrigerant is at 10.3 bar, corresponding to the saturation pressure of R-410A at 8.3°C. Upon startup, the compressor motor ramps up to its maximum value of 3500 RPM. The refrigerant rapidly migrates from the low pressure side to the high pressure side. This causes a sharp decrease in the suction pressure and a corresponding increase in the discharge pressure for the first two minutes. The compressor mass flow rate quickly peaks, as seen in Figure 4(e). As refrigerant continues to migrate to the high pressure side, the density of the refrigerant in the low-pressure side decreases. Thus, the density of the vapor entering the compressor drops, causing a decrease in the mass flow rate after the initial maxima.

The refrigerant flow through the valve takes longer to establish in comparison to the compressor. Two phenomena dictate the valve flow rate: the pressure difference across the valve and the inlet liquid density. Initially, the indoor coil does not fully condense the refrigerant to subcooled state, and thus the inlet density is low. Further, the pressure difference across the valve is smaller, and thus the flow through the valve is small. Once the mass flow rate through the valve starts to increase, however, the rate of pressure change slows down. It is seen in Figure 4(a) that, in six minutes, the system does not attain steady state and the pressures are still evolving.

A comparison of the temperatures is given in Figure 4(b). Upon startup, the discharge temperature increases sharply to around 60°C and then decreases slightly. After shutdown, the discharge temperature in the test setup is seen to decrease instantaneously down to the saturation temperature before increasing. This is attributed to the static head created by the indoor unit (condenser) being placed much higher than the compressor. After shutdown, the refrigerant flow through the compressor ceases immediately. Thus, the liquid within the condenser migrates in the reverse direction as the compressor driven flow due to gravity. The models do not account for gravity and thus cannot capture this phenomenon. Instead, the simulations show a gradual decay of temperature approaching the ambient conditions as the compressor continues to lose heat through natural convection and radiation.

The air outlet temperatures are shown in Figure 4(c) for both the indoor and the outdoor coils and match the experimental trends well during the on-period. During the off-period, the outdoor unit fan is turned off, while the indoor unit air (circulated using the closed air loop blower) stays on. The off-cycle indoor coil air temperature predictions for both the platforms evolve faster than measured data. This is due to the models not incorporating the thermal inertia of the closed air loop, which continues to retain heat. The heating up of the outdoor coil air is also not as significant in the simulations as in the experimental data, and this is due to the simulations not accounting for the heat transfer from the hot compressor being located *inside* the outdoor unit.

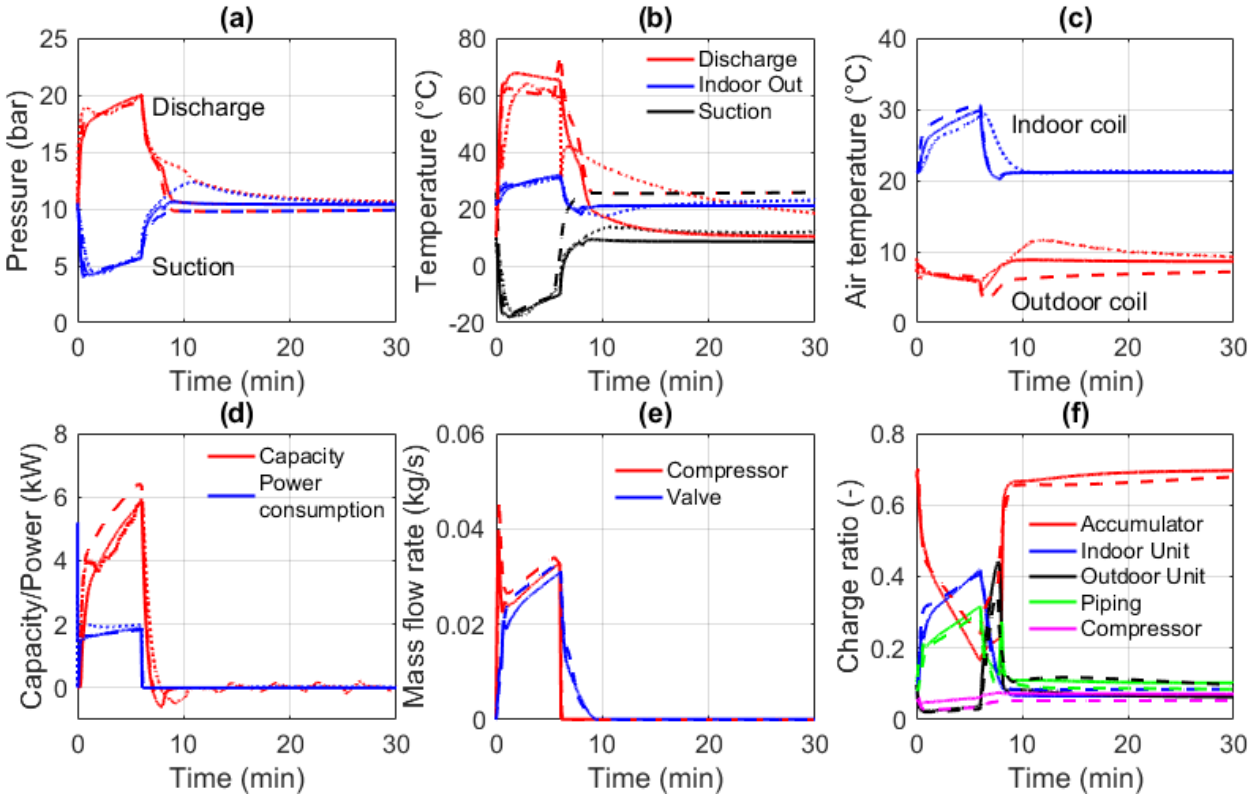

Figure 4. R-410A High Temperature Cyclic test. (a) Refrigerant pressures (b) Refrigerant temperatures (c) Air outlet temperatures (d) Capacity and power consumption (e) Mass flow rates (f) Refrigerant charge distribution. *(Dotted lines are measured data, dashed lines are Dymola data and solid lines are EcosimPro data)*

The compressor power consumption and the indoor unit air side capacities are shown in Figure 4(d). These parameters help to quantify the performance of the heat pump, and can be used to investigate the cycling losses and the energy

efficiency ratio of the system. The cyclic capacity is predicted fairly well by the models. The power consumption is also predicted well, although the assumption of constant isentropic efficiency of compressor leads to a slight mismatch in the initial stages of the on-period.

The refrigerant charge distribution shown in Figure 4(f) indicates that during the on-period, nearly a quarter of the system charge resides in the piping (primarily in the long liquid lines). Thus, it is important to account for this volume of charge. After the off period, the refrigerant initially migrates towards the outdoor unit and eventually, only vapor is present in the indoor unit. After about 8 minutes, the charge shifts into the accumulator and the migration stabilizes at around ten minutes.

5.2 Cooling Mode Results

The cooling mode results are shown in Figure 5. It can be observed that some of the system characteristics such as the refrigerant temperatures and pressures, largely resemble the heating mode. The differences in transients between the two modes arise mainly due to the presence of a TXV in the cooling mode.

The mass flow rate through the TXV, shown in Figure 5(e), reaches a maximum in the initial stages and then decreases. This is caused by the thermal inertia of the sensor bulb of the valve. In the initial stages, the refrigerant rapidly migrates from the evaporator, reducing the suction pressure. However, the sensor bulb pressure (dictated by the bulb temperature), takes time to adapt due to the thermal resistances of the piping and the sensor bulb as well as the contact between them. Thus, a pressure imbalance is created on the diaphragm which forces the valve open. Once the bulb begins to respond, however, the valve begins to control the superheat, and a subsequent reduction in mass flow rate is seen.

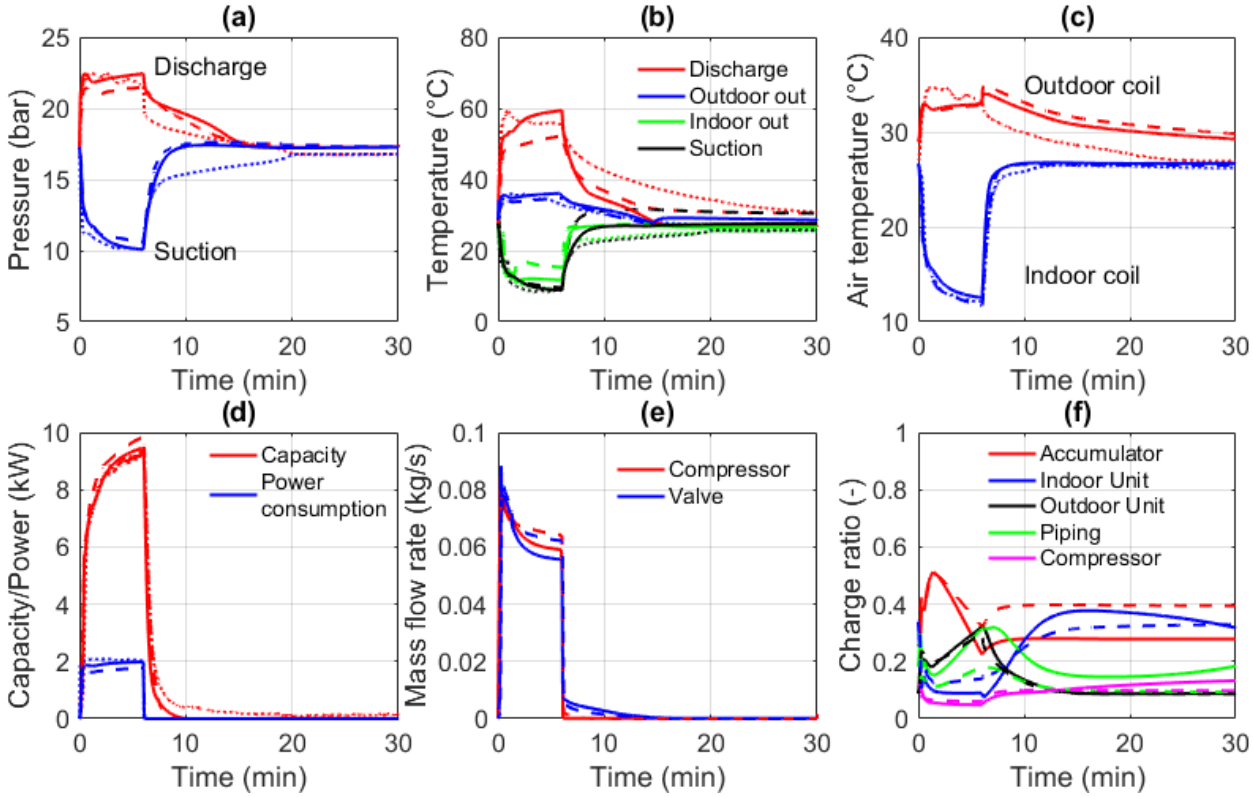

Figure 5. R-410A D test (a) Refrigerant pressures (b) Refrigerant temperatures (c) Air outlet temperatures (d) Capacity and power consumption (e) Mass flow rates (f) Refrigerant charge distribution. *(Dotted lines are measured data, dashed lines are Dymola data and solid lines are EcosimPro data)*

For the cooling mode, the Dymola simulations required 5098 seconds for completion, while the EcosimPro simulations were completed within 1324 seconds. The differences in simulation times are caused mainly by the different fluid property routine methods adopted and providing a numerically small refrigerant flow in EcosimPro

instead of an exact zero flow during the off-cycle in Dymola. The ability to simulate true zero flow conditions allows for a more robust calculation scheme in conditions where repeated on-off cycling occurs, for instance in systems featuring multiple evaporators for multiple zones.

5.3 Cycling Losses Comparisons

The accumulated capacities and power consumption (integrated values during the on cycle in W-hr) are often used to quantify the deviations between measured and simulated systems. These values are listed in Table 3. It can be seen that both platforms are able to predict these parameters within 20% of the measured values.

The ability to perform such analyses can be useful in investigating 'what-if' scenarios. In the cooling case, the charge in the off-cycle migrates to the indoor unit, which is the coldest part of the cycle. This migration causes cycling losses, (discussed in detail by Kapadia et al. (2009)). System designers have attempted to handle such losses by using methods such as employing a non-bleed TXV which completely shuts off without leakage during the off cycle, and prevents high pressure refrigerant from losing energy (J. Wang & Wu, 1990). Such designs could feasibly be investigated using the current models, by calculating the differences in accumulated capacities between the non-bleed and traditional TXVs and comparing the Heating and Cooling Load Factors.

Table 3. Cycling losses analysis

	Experimental	**Dymola**		**EcosimPro**	
		Value	% Error	Value	% Error
D test					
Accumulated capacity (W-hr)	779.67	837.65	7.4%	802.09	2.9%
Accumulated power consumption (W-hr)	203.29	162.94	-19.8%	186.50	-8.25
High Temperature Cyclic test					
Accumulated capacity (W-hr)	420.19	503.74	19.8%	412.23	-1.9%
Accumulated power consumption (W-hr)	192.89	165.52	-14.2%	167.34	-13.2%

6. CONCLUSIONS

Two object-oriented physical modeling platforms, Dymola and EcosimPro, have been compared. A relatively complex residential heat pump was simulated and validations were conducted against experimental data. Both platforms showed good capabilities in predicting the transient behavior of the system. A wide variety of parameters could be investigated: refrigerant pressures and temperatures, heat exchanger capacities, compressor power consumption and the charge distribution within individual components. The EcosimPro platform showed faster simulation speed through the use of lookup tables to calculate the fluid property routines, whereas the Dymola models utilize detailed property routines and are able to simulate a true zero-flow condition.

NOMENCLATURE

A	Area	m^2	T	Temperature	K
Cp	Specific heat capacity	W/kg.K	u	Specific internal energy	J/kg
h	Density-weighted enthalpy	J/kg	V	Volume	m^3
$\dot{m}$	Mass flow rate	kg/s	x	Static vapor quality	-
p	Pressure	bar	ρ	Density	kg/m^3
Q	Heat transfer rate	W	η	Efficiency	-

Subscripts

0	Design (nominal) values
in	Inlet
i,j	Control volume indexes
out	Outlet
v	Volumetric (efficiency)
w	Wall

REFERENCES

Alabdulkarem, A., Hwang, Y., & Radermacher, R. (2013). *Test Report #20 System Drop-In Tests of Refrigerants R-32, D2Y-60, and L-41a in Air Source Heat Pump*. Arlington, VA.

ASHRAE. (2010). Methods of Testing for Seasonal Efficiency of Unitary Air-Conditioners and Heat Pumps. *ASHRAE Standard 116-2010*. Atlanta, GA: ASHRAE.

Aute, V., & Radermacher, R. (2014). Standardized Polynomials for Fast Evaluation of Refrigerant Thermophysical Properties. In *15th International Refrigeration and Air Conditioning Conference*. West Lafayette, IN: Purdue University.

Bhanot, V., Ling, J., Aute, V., & Radermacher, R. (2016). Simulink Based Transient Modeling of a Flash Tank Vapor Injection System and Experimental Validation. In *16th International Refrigeration and Air Conditioning Conference*. West Lafayette, IN: Purdue University.

Churchill, S. W., & Chu, H. H. S. (1975). Correlating Equations for Laminar and Turbulent Free Convection from a Vertical Plate. *International Journal of Heat and Mass Transfer*, *18*, 1323–1329.

Dermont, P., Limperich, D., Windahl, J., Prölss, K., & Kübler, C. (2016). Advances of Zero Flow Simulation of Air Conditioning Systems using Modelica. In *Proceedings of the 1st Japanese Modelica Conference* (pp. 139–144). Tokyo. https://doi.org/10.3384/ecp16124139

Eldredge, B. D., Rasmussen, B. P., & Alleyne, A. G. (2005). Vapor compression cycles: control-oriented modeling and validation. In *ASME 2005 International Mechanical Engineering Congress and Exposition* (pp. 1213–1222).

Elmqvist, H., Mattsson, S. E., & Otter, M. (1999). Modelica-a language for physical system modeling, visualization and interaction. In *Proceedings of the 1999 IEEE International Symposium on Computer Aided Control System Design* (pp. 630–639). Kohala Coast, Hawaii, USA. https://doi.org/10.1109/CACSD.1999.808720

Hossin, K., Mahkamov, K., Belgasim, B., Hashem, G., & Elsharif, N. (2001). Thermodynamic Performance Investigation of a Small-Scale Hybrid Solar-Biomass Power System Based on Organic Rankine Cycle. *Applied Thermal Engineering*, *21*, 381–390.

Kapadia, R. G., Jain, S., & Agarwal, R. S. (2009). Transient Characteristics of Split Air-Conditioning Systems Using R-22 and R-410A as Refrigerants. *HVAC&R Research*, *15*(3), 617–649.

Lemmon, E. W., Huber, M. L., & McLinden, M. O. (2013). NIST Standard Reference Database 23: Reference Fluid Thermodynamic and Transport Properties-REFPROP, Version 9.1, National Institute of Standards and Technology. Gaithersburg: National Institute of Standards and Technology. https://doi.org/http://dx.doi.org/10.18434/T4JS3C

Ling, J., Bhanot, V., Alabdulkarem, A., Aute, V., & Radermacher, R. (2015). Transient simulation of heat pumps using low global warming potential refrigerants. *Science and Technology for the Built Environment*, *21*(5), 658–665. https://doi.org/10.1080/23744731.2015.1034044

Muñoz, L., Vara, R., Bencomo, S., & Soria, M. (2003). Comparison between Modelica 2.0 and EcosimPro/EL 3.2. *2nd Meeting of EcosimPro Users, UNED*, (February), C207(1)-C207(11).

Petzold, L. (1982). Differential/Algebraic Equations Are Not ODE's. *Journal of Scientific and Statistical Computing*, *3*(3), 367–384. https://doi.org/10.1137/0903023

Qiao, H., Aute, V., & Radermacher, R. (2012). Comparison of Equation-based and Non-equation-based Approaches for Transient Modeling of a Vapor Compression Cycle. In *International Refrigeration and Air Conditioning Conference*.

Qiao, H., Aute, V., & Radermacher, R. (2015). Transient modeling of a flash tank vapor injection heat pump system - Part I: Model development. *International Journal of Refrigeration*, *49*, 169–182. https://doi.org/10.1016/j.ijrefrig.2014.06.019

Wang, C. C., Chi, K. Y., & Chang, C. J. (2000). Heat transfer and friction characteristics of plain fin-and-tube heat exchangers, part II: Correlation. *International Journal of Heat and Mass Transfer*, *43*(15), 2693–2700. https://doi.org/10.1016/S0017-9310(99)00333-6

Wang, J., & Wu, Y. (1990). Start-up and shut-down operation in a reciprocating compressor refrigeration system with capillary tubes. *International Journal of Refrigeration*, *13*(3), 187–190. https://doi.org/https://doi.org/10.1016/0140-7007(90)90074-7

Winkler, J. M. (2009). *Development of a Component Based Simulation Tool for the Steady State and Transient Analysis of Vapor Compression Systems*. University of Maryland, College Park. Retrieved from http://drum.lib.umd.edu/handle/1903/9139